Performances Study of a Hybrid Rocket Engine

Adrian-Nicolae BUTURACHE*,[1,a]

*Corresponding author
*The Bucharest University of Economic Studies,
Doctoral School of Economic Cybernetics and Statistics,
11st Tache Ionescu Street, 010351, Bucharest 1, Romania,
ad.buturache@yahoo.ro
[1]"POLITEHNICA" University of Bucharest, Faculty of Aerospace Engineering,
1-7 Polizu Street, 011061, Bucharest 1, Romania

DOI: 10.13111/2066-8201.2018.10.2.16

Received: 16 February 2018/ Accepted: 05 May 2018/ Published: June 2018

Abstract: *This paper presents a study which analyses the functioning and performances optimization of a hybrid rocket engine based on gaseous oxygen and polybutadiene polymer (HTPB). Calculations were performed with NASA CEA software in order to obtain the parameters resulted following the combustion process. Using these parameters, the main parameters of the hybrid rocket engine were optimized. Using the calculus previously stated, an experimental rocket engine producing 100 N of thrust was pre-dimensioned, followed by an optimization of the rocket engine as a function of several parameters. Having the geometry and the main parameters of the hybrid rocket engine combustion process, numerical simulations were performed in the CFX – ANSYS commercial software, which allowed visualizing the flow field and the jet expansion. Finally, the analytical calculus was validated through numerical simulations.*

Key Words: *rocket, propellant, hybrid, thrust, numerical simulation*

1. INTRODUCTION

The first rocket propelled by a hybrid rocket engine belongs to Sergei Korolev, and flew on 3rd of August 1933 [1]. Named GRID09, the rocket produced 500 N of thrust and reached an altitude of 1500 meters. The oxidizer used was liquid oxygen, which is used also in our days. The solid state fuel was a mixture between crude oil and rosin (colophony). Organizations from German influenced states and from USA, which intended to study rocket engines, continued testing rocket engines on a small scale, this including the tests conducted by Hermann Oberth near Vienna in 1938 and 1939, using liquid oxygen as an oxidizer, while the solid state fuel was a mixture of tar, wood and potassium nitrate. Other options for the solid fuel in those times were the coal and the wood.

After WW2, the first mention regarding the use of polyethylene as a solid fuel occured in 1951 in USA. In this case the oxidizer was hydrogen peroxide. Then, the development continued in USA, France and Germany, evaluating and recording numerous combinations of oxidizers and solid fuels, used still on small scale rocket engines.

[a] PhD. Eng.

The combination of metallic powders (lithium) and solid fuel and the use of exotic oxidizers like mixtures of fluorine and liquid oxygen, or ionic thrusters [16, 21] led to obtaining rocket engines producing high thrusts.

Notable results in this domain were obtained in USA by United Technologies Corporation (UTC). The rocket engines produced by UTC reached thrusts of tens of kilonewtons. This leap allowed the manufacturing of the Dolphin, launched at sea, having an engine producing 175 kN of thrust which used as propellants liquid oxygen and polybutadiene. AMROC Company tested a series of hybrid rocket engines producing thrusts up to 324 kN. In this case, the propellants used were also the liquid oxygen and the polybutadiene [2].

The aim was to realize a space launcher, but, because of the SET-1 failure whose engine developed a thrust in vacuum of 931 kN and could carry 25 tons of propellant, AMROC ceased its activity, and SpaceDev overtook and carried on what the latter ones have already started. The rocket engine with hybrid fuel delivered by SpaceDev which equips SpaceShip One produces a thrust of 74 kN using 2,4 tons of propellant [3].

The use of hybrid rocket engines is becoming more and more popular, especially in the space tourism industry. [4, 5]. A series of theoretical and experimental researches were developed over the time [6, 7, 8].

In this paper a calculus for a hybrid propelled rocket producing 100 N of thrust will be conducted in order to assess the replacement of the actual solid propellant which has low specific impulses and produces dangerous fumes following the combustion process, but also of the liquid propellants which need complex distribution systems.

2. ADVANTAGES AND DISADVANTAGES OF THE HYBRID FUEL ROCKET ENGINES

Several advantages and defining features of the hybrid rocket engines are listed as follows:

1. *Safety.* The solid fuel is inactive and it can be produced, transported and manipulated according to the standard commercial practices. The hybrid rocket engine does not involve an explosion hazard due to the fact that the mixture between oxidizer and solid fuel is delivered only in a controlled, programmed manner.

2. *Simple acceleration, deceleration and stop.* Hybrid rocket engines can be accelerated or decelerated by adjusting the oxidizer flow (the classic hybrid rocket engine), operation which is simpler than the liquid rocket engines where the flows must be adjusted and synchronized all the time, both for the oxidizer and the liquid fuel. In the case of the hybrid rocket engine, the *O/F* ratio, which results following the vaporization of the solid fuel surfaces layer by layer, is adjusted depending on the evolution of the oxidizer flow. Thus, the thrust of the rocket engine is decreased by reducing the oxidizer flow, and by completely reducing this flow, the engine is shut down completely, this being an important factor in order to stop the hybrid rocket engine.

3. *Robustness of the load.* Unlike the solid fuels used in solid rocket engines, eventual cracks won't represent a danger due to the fact that the combustion process begins in the area where the oxidizer is injected.

4. *Fuel versatility.* In order to select the solid fuels and the oxidizers, when compared with solid and liquid fuel rocket engines, hybrid rocket engines offer more possible combinations. Compared to the liquid rocket engines, metallic powders can be added in the solid fuel to increase both its density and performances. Also, when compared to the solid rocket engine, the liquid state oxidizers ensure much higher energetic levels.

5. *Sensitivity to temperature variations.* Due to the fact that the effect of the temperature over the combustion speed is small, as in the case of the liquid fuel rocket engine, the variation of the ambient temperature has a low impact over the pressure in the combustion chamber.

Thereby, in the case of solid fuel rocket engine an aspect of interest is linked to the maximum operating pressure and, also, how the pressure evolves depending on the environment conditions.

6. *Low cost.* The total operating costs of the hybrid rocket engine decrease significantly due to its characteristics which offer safety in exploitation and due to the inactive fuel. The fuel production can be made in commercial, civil facilities, which don't need a special infrastructure, like when producing fuels for the solid fuel rocket engines. As a consequence, the factories can be placed near the launch sites. More than that, the hybrid rocket engine has a wide range of possibilities regarding the calculus and the design, once again resulting low costs for production [9, 10].

7. *Green propellant.* The chemical products resulted following the combustion reaction of the most advanced solid fuels contain important traces of hydrochloric acid and other hazardous substances.

There are a lot of studies regarding the development of new propellants which are more environmental friendly [11].

Obviously, this series of advantages comes also with a series of disadvantages presented below:

1. *Low regression rate.* In order to ensure the combustion area necessary to reach the desired thrust, most of the combustion load must have multiple combustion apertures and dimensions which frequently overcome 300-400 [mm]. These characteristics are suitable for applications which involve large operating periods and low thrusts.

2. *Low density.* A consequence of the low regression rate is that a large combustion surfaces is needed to ensure the desired thrust. This condition is fulfilled, in general, by using solid fuel loads with multiple apertures which finally lead to a low specific mass. The number of sharp edges in a load with multiple apertures leads to fuel strips which remain unburned.

However, the research conducted lately led to the increase of the regression rate and thus to the decrease of the effects of this drawback.

3. *Combustion efficiency.* The diffusive nature of the flames leads to a low quality of the mixture and, thereby, to a low efficiency regarding the specific impulse. This type of loss is, in general, larger by 1-2% than for the solid or liquid fuel rocket engine. However, when compared to the solid fuel rocket engine, the performance delivered by the engine is larger due to the larger specific impulse, I_{sp}.

4. *Change of the O/F ratio.* Increasing the diameter of the combustion aperture during the combustion process leads, obviously to the modification of the *O/F* ratio throughout the combustion process. This fact has as a consequence the decrease of the hybrid rocket engines performances. However, using a suitable approach of the problem generated by the *O/F* ratio, the performance decrease is minimum, and the ballistic calculus shows that this decrease can have values as low as up to 1% for a classic hybrid rocket engine.

5. *Slow transitions.* The transient regime during the ignition phase is slow, so the thrust modification during the engine speed up is low, too. In practice, the repeatability of ignitions and accelerations are way more important, so the reaction speed comes on a second place [9, 10].

3. PROPELLANT SELECTION

Due to the fact that the purpose of this paper is to approach problems related to the low regression rate of the hybrid rocket engines in several configurations, it is useful to analyze some of the performances and basic applications of the hybrid rocket engines in order to ensure that the details linked to the regression rate are put in the right context. In the early days of studying the combustion in hybrid rocket engines, wood, wax and other types of hydrocarbons were used. Although the acryl and the polyethylene are sometimes used for the laboratory experiments, at this moment the most used fuels are those based on butadiene, like HTPB [12, 13, 14]. HTPB is safe, easy to obtain, being a polymer made of a mixture between resin and curing agent. This mixture can be easily enhanced by adding agents to increase the mechanical strength of the load, agents to increase the density, carbon powders to obtain opaque surfaces which stop the penetration of the thermal radiation or metallic powders to increase the energy resulted following the combustion process [15].

Rocket engines using HTPB as a solid fuel obtain a specific impulse larger than the solid fuel rocket engines, e.g. ammonium perchlorate/HTPB, but smaller than the liquid fuel rocket engines, e.g. LO_2 / LH_2.

However, HTPB/LOX ensures performances close to the LOX/kerosene combination. On the other side, hybrid rocket engines using solid fuels based on polybutadiene have a higher specific impulse than the solid fuel rocket engines, but lower than the liquid fuel rocket engines. The figure below presents the dependency of the specific impulse on the (O/F) ratio for a pressure of 1000 PSI in the combustion chamber and a ratio between the outlet cross section and the critical section of the nozzle of 10:1.

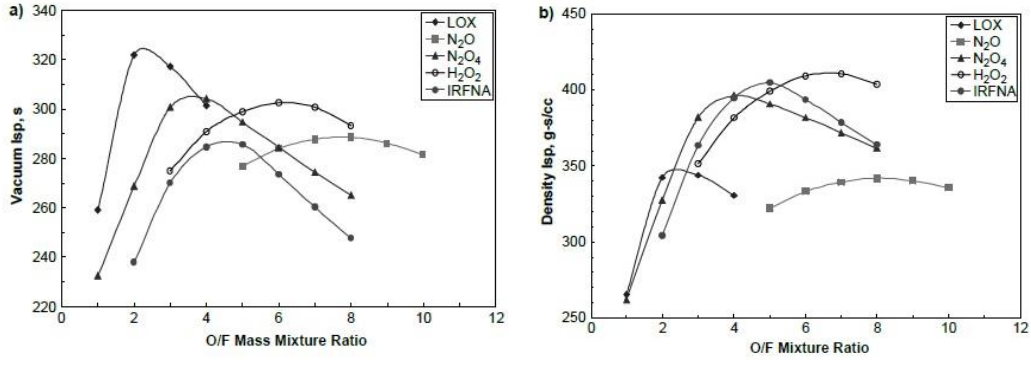

Fig.1 - a. Specific impulse as a function of the O/F ratio, considering the oxidizer's density, b. Specific impulse as a function of the O/F ratio [16, 17]

An important mention is that LOX offers the highest specific impulse due to the high oxidizing potential, while the oxygen peroxide (H_2O_2) ensures a high specific mass [18].

4. PERFORMANCES ANALYTIC CALCULUS OF A HYBRID ROCKET

The dynamic behavior of the hybrid rocket engine can be analyzed using the continuity equation as written below:

$$\frac{\partial(\rho_1 V_1)}{\partial t} = \dot{m}_{in} - \dot{m}_{out} \tag{1}$$

This shows the difference between the oxidizer flow entering the working aperture plus the fuel generated following the sublimation of the solid state load and the propellant flow exiting the nozzle. This relation can be written as follows:

$$\frac{\partial(\rho_1 V_1)}{\partial t} = \dot{m}_o + \dot{m}_f - \frac{p_1 A_t}{c^*} \tag{2}$$

where A_t is the cross section area, and c^* is the characteristic speed; c^* can be written as:

$$c^* = \frac{p_I A_t}{\dot{m}} = \frac{\sqrt{kRT_1}}{k\sqrt{\left[\frac{2}{(k+1)}\right]^{\frac{(k+1)}{(k-1)}}}} \tag{3}$$

When the stationary regime is reached, them flow equation can be written as:

$$\dot{m} = \dot{m}_o + \dot{m}_f = \frac{p_1 A_t}{c^*} \tag{4}$$

The expression of the hybrid rocket engine thrust can be written as follows:

$$F = \dot{m} I_s g_0 = \left(\dot{m}_0 + \dot{m}_f\right) I_s g_0 \tag{5}$$

The fuel flow can be written as a function of its nature (density), geometry (combustion surface area, which is obviously obtained knowing the length of the load and the diameter of the cross section) and the regression rate.

$$\dot{m}_f = \rho_f A_b r = 2\pi\rho_f RLr \tag{6}$$

where A_b is the combustion surface area and L the length of the load.

The initial flows of fuel and oxidizer:

$$\dot{m} = \dot{m}_o + \dot{m}_f = \dot{m}_f \left(\frac{O}{F} + 1\right) \tag{7}$$

Knowing the initial diameter of the working aperture, the speed of the mass flow of the oxidizer can be written as:

$$G_0 = \frac{\dot{m}_o}{NA_p} \tag{8}$$

where A_p is the diameter of the working aperture.

The regression rate at the initial moment can be expressied using equation (5):

$$r_{HTPB} = 0.104 G_0^{0.681} \tag{9}$$

The length of the solid fuel load:

$$L = \frac{\frac{m_f}{N}}{2\pi R_i \rho_f r} \tag{10}$$

The specific impulse:

$$I_s = \frac{C_F c^*}{g_0} \tag{11}$$

In order to determine the geometry of the nozzle, the calculus started from the combustion temperature of the propellants and the pressure imposed in the combustion chamber, the temperatures and pressures in the critical and outlet section were calculated using the thermogas dynamics equations for temperature and pressure.

The flow was calculated as a function of the critical section area. Starting from calculating the thrust coefficient:

$$C_f = \sqrt{\frac{2\gamma}{\gamma-1}\left(\frac{2}{\gamma+1}\right)^{\frac{\gamma+1}{\gamma-1}}\left[1-\left(\frac{p_e}{p_c}\right)^{\frac{\gamma-1}{\gamma}}\right]} \tag{12}$$

The expression used to calculate the flow is:

$$\dot{m} = \sqrt{\frac{\gamma}{MW}}\frac{p_c}{\sqrt{T_c}}\frac{A_t}{\left(\frac{\gamma+1}{2}\right)^{\frac{\gamma+1}{2(\gamma-1)}}} \tag{13}$$

where MW is the mollecular mass of the propelants mixture.

The outlet section area is calculated using the following expression:

$$A_e = \frac{A_t M_t\left(1+\frac{\gamma-1}{2}M_t^2\right)^{\frac{\gamma+1}{2(\gamma-1)}}}{M_e\left(1+\frac{\gamma-1}{2}M_t^2\right)^{\frac{\gamma+1}{2(\gamma-1)}}} \tag{14}$$

where M_e is the Mach numbers obtainer at the nozzle exit, and it is obtained from:

$$M_e = \sqrt{\frac{2}{\gamma-1}\left[\left(\frac{p_c}{p_{atm}}\right)^{\frac{\gamma-1}{\gamma}}-1\right]} \tag{15}$$

In the first phase the profiled nozzle was a conical shaped one. The profiling started from the divergence angle of the cone nozzle $\theta = 30^\circ$ $\left(\alpha = \frac{\theta}{2} = 15^\circ\right)$, then the length of the conical section, L, was calculated, and also the radius of the arc which generates the critical section zone, R.

$$L_{cone} = \frac{r_e - r_t}{\tan\theta} \tag{16}$$

where r_e and r_t are the radius of the outlet and critical section.

In order to conduct the calculus, the following parameters were imposed: thrust F=100 N and pressure inside the combustion chamber 20 bar.

In order to determine the physical-chemical properties for the propellants mixture used, the Chemical Equilibrium with Applications (CEA) was used [19]. The following results were obtained:

Table 1

O/F ratio value	Flame temperature [K]	Propellant density $\left[\frac{kg}{m^3}\right]$	Specific heats ratio	Molar mass $\left[\frac{kg}{kmol}\right]$
3,25	3529	0,8523	1,1253	25,008

Table 2

Oxidizer flow $\left[\frac{kg}{s}\right]$	Fuel flow $\left[\frac{kg}{s}\right]$	Regression rate $\left[\frac{mm}{s}\right]$	Fuel load length $[m]$	Specific impulse $[s]$	Critical section diameter $[m]$
0,0329	0,0101	1,3401	0,2027	237,1048	0.0066
Outlet section diameter $[m]$	Critical section temperature $[K]$	Outlet section temperature $[K]$	Critical section pressure $[Pa]$	Outlet section pressure $[Pa]$	Exhaust speed $\left[\frac{m}{s}\right]$
0,0132	$2,9985 \cdot 10^3$	$2,2701 \cdot 10^3$	$1,1985 \cdot 10^6$	$1.013 \cdot 10^5$	2325,9977

After applying the mathematical model, starting from the values imposed initially, the following parameters of interest were obtained:

For the temperature inside the combustion chamber, a coefficient, η, is applied, which considers the imperfections occurred during the combustion process, but also the losses during the transition between the combustion chamber and the entry in the nozzle.

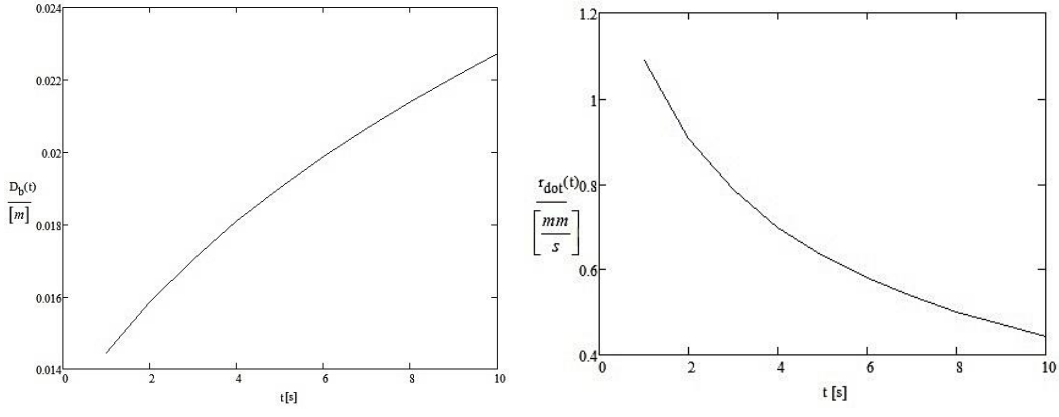

a b

Fig. 2 - a) The evolution in time of the inner diameter of the solid fuel load,
b) The evolution in time of the regression rate

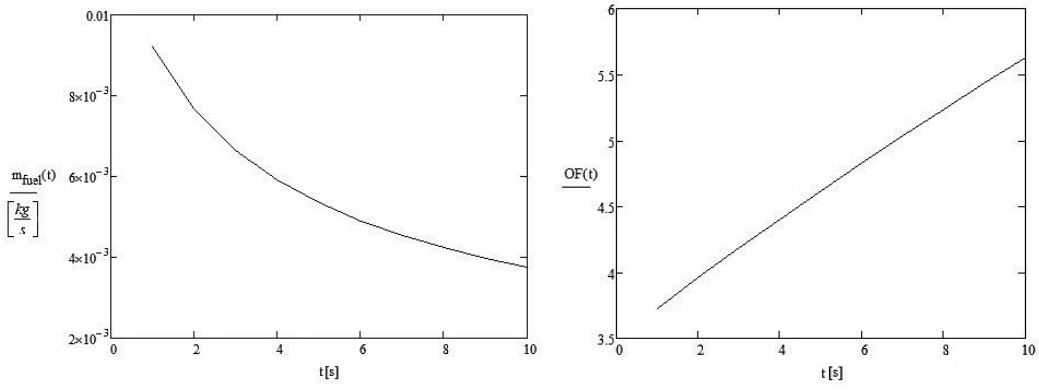

a b

Fig. 3 - a) The evolution in time of the fuel flow, b) The evolution in time of the O/F ratio

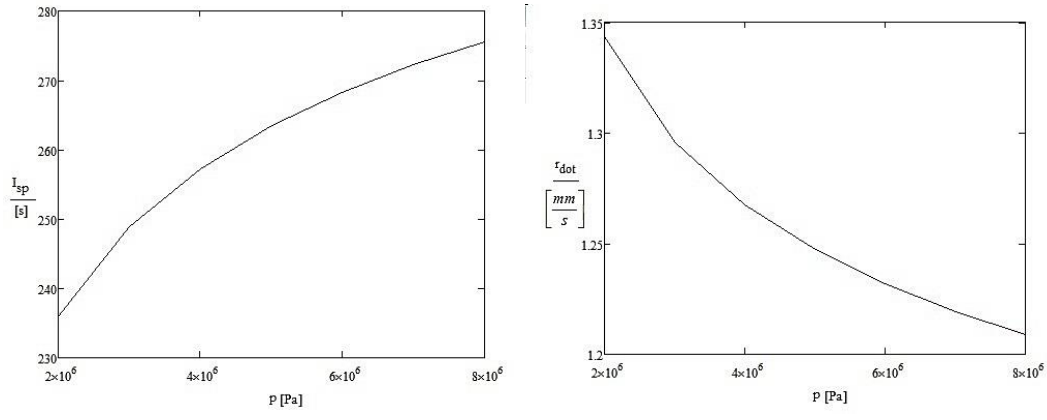

a b

Fig. 4 - a) Specific impulse as a function of the pressure inside the combustion chamber, b) Regression rate as a function of the pressure inside the combustion chamber

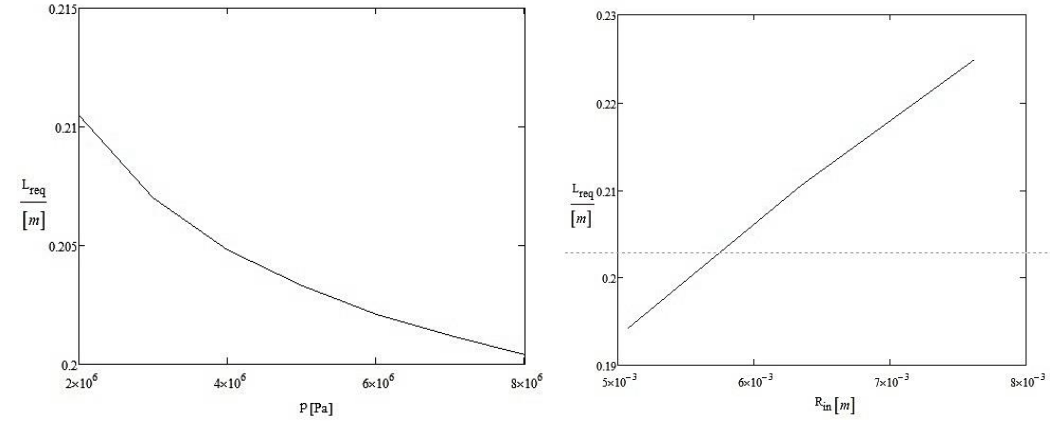

a b

Fig. 5 - a) The length of the solid fuel load as a function of the pressure inside the combustion chamber, b) The length of the solid fuel load as a function of its inner radius

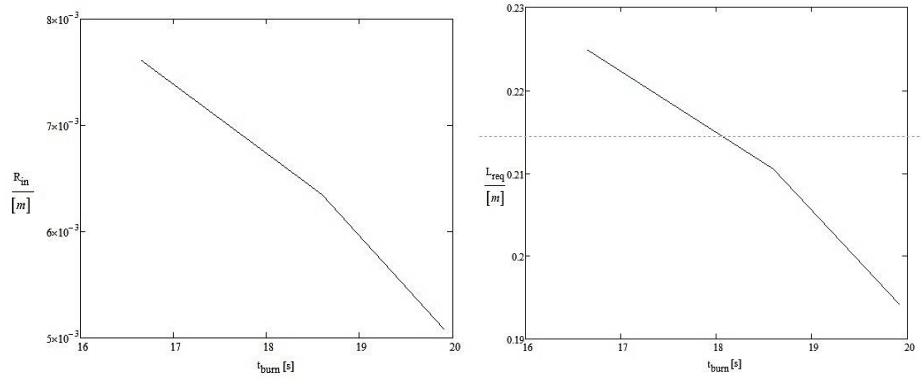

a b

Fig. 6 - a) The burning time as a function of the inner diameter of the solid fuel load (the final radius of the solid fuel load is constant), b) The burning time as a function of the length of the solid fuel load (the final radius of the solid fuel load being constant)

5. CFX SIMULATIONS AND COMPARISON OF THE RESULTS

Using the analytical results, the geometrical dimensions led to mesh generation.

The flow field length for the jet expansion is equivalent to 30 exit nozzle diameters on axial direction and 5 exit nozzle diameters on radial direction. The calculus grid was produced in commercial software by using only a structured mesh.

Knowing that the field is axially symmetric, one considers only the computational domain comprising an angle of 90 degrees, so having a 3D domain.

In this way we could introduce more elements in the field related to the power of the computer. In this sector of the field 624,000 nodes are used. Thus, the entire area has a total of almost 2.5 million nodes.

In the figure below one observes how this mesh is formatted and structured.

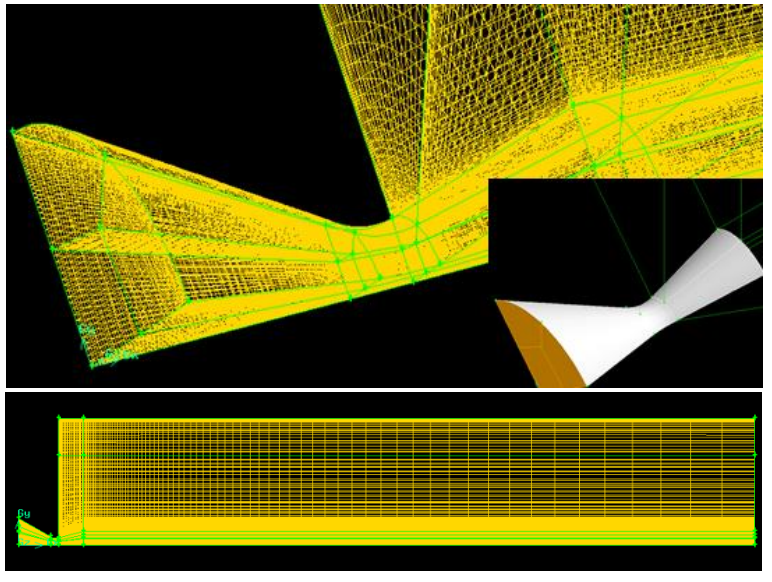

a

b

Fig. 7 - Structured mesh and detail of the nozzle sector

The coordinates system: the Ox axis is directed downstream and the Oy axis is radial.

The chosen working fluid was an ideal gas, the inlet parameters being the ones calculated for the combustion gases of the propellant chosen for this study.

The boundary conditions have an important role in the description of the behavior of complex flows. Usually, these conditions are chosen so that the model can reproduce the real phenomenon.

One takes into consideration the following boundary conditions:

- Mass flow inlet;
- Opening;
- At the left and right sides of computational domain, the rotational periodic boundary;

Following the calculus of the Reynolds Number which has a value of about10 to the power -6 one considers that the flow is turbulent and the chosen model of turbulence is k-ε. The values of k and ε come from the transport equation of the turbulent kinetic energy and the turbulent dissipation.

In order to validate the CFX results, the parameter y + must have the values below 30 and above 30.

The numerical simulations were performed with commercial CFX code Ansys 15 [20]

The figures below presents the most important field parameters:

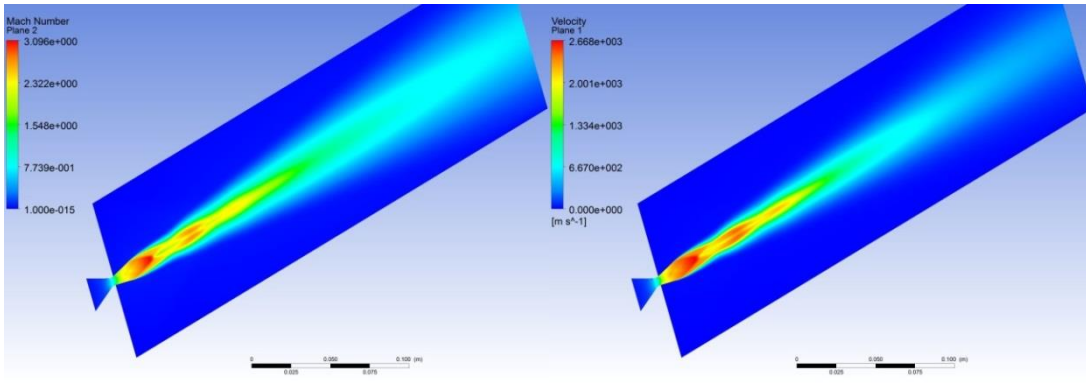

a b

Fig. 8 - Flow field, a. Mach number, b. Speed

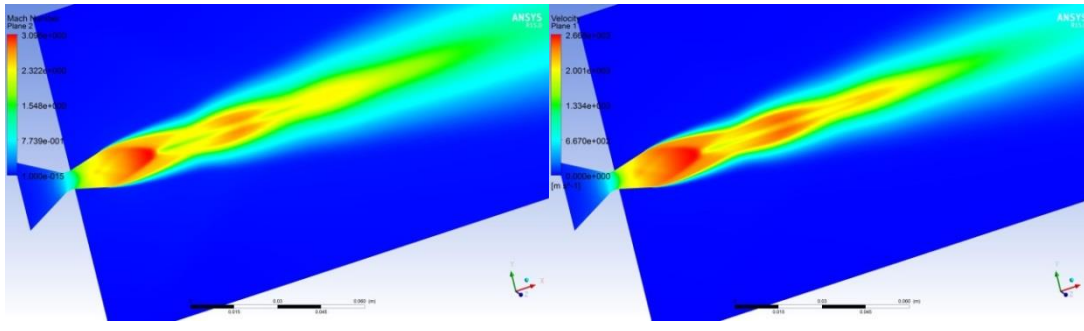

a b

Fig. 9 - Detailed graphical representation of the flow field, a. Mach number, b. Speed

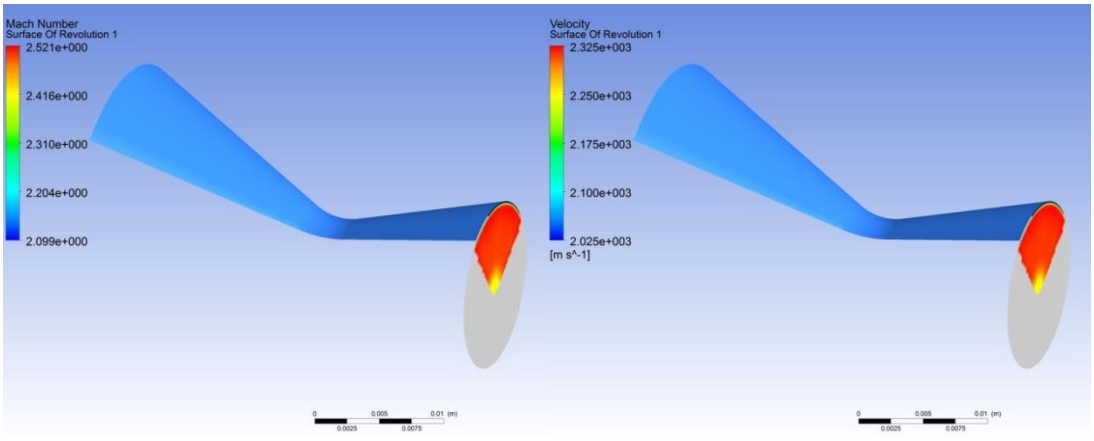

a b

Fig. 10 - Flow field, a. Mach number read in the nozzle outlet cross section, b. Speed

After running the obtained hybrid rocket geometry in CFX, parameters of interest were read, like speed and Mach number in the outlet section, observing that the average value in the outlet section for the seed was 2306 m/s, and the Mach number 2.4945.

6. CONCLUSIONS AND DISCUSSIONS

It can be observed that, throughout its increasing, the pressure inside the combustion chamber produces a raise of the specific impulse, but also a decrease of the fuel flow. The decrease of the fuel flow, given the fact that the O/F ratio is considered steady, leads to the decrease of the oxidizer flow. The oxidizer flow influences the regression rate throughout the value of the mass flow unit, in this case by increasing the pressure inside the combustion chamber, the regression rate decreases, too. For the same quantity of solid fuel, but with a variation of the inner radius of the solid fuel load, the theoretical burning time of the solid fuel load varies also.

The same situation is found also in the case of varying the length of the solid fuel load. In order to have a constructive solution which can also be tested, a balance between the imposed parameters and the desired results shall be found. Any increase in the pressure of the combustion chamber will, obviously, produce an increase of the techological problems in terms of complexity.

After running the geometry of the hybrid rocket in CFX, it can be observed the flow field, both inside the reactive nozzle, and in the expanding domain of the produced jet.

Parameters of interest like speed and Mach number in the outlet section were read, observing that the average value in the outlet section for the seed was 2306 m/s, and the Mach number 2.4945.

Following the analytic calculus, the speed in the outlet section was 2356 m/s, and the Mach number was 2.52, so it can be concluded that the analytical results were correctly validated throughout numerical calculus using CFX.

Considering the analytic model validated can represent a starting point for dimensioning a hybrid rocket engine which offers an alternative worthy of consideration in order to replace the solid and liquid fuel rocket engines.

REFERENCES

[1] A. A. Chandler, B. J. Cantwell, G. Scott Hubbard, A. Karabeyoglu, Feasibility of a single port Hybrid Propulsion system for a Mars Ascent Vehicle, *Acta Astronautica*, Volume **69**, Issues 11–12, December 2011, Pages 1066–1072.

[2] G. Story, *Large-Scale Hybrid Motor Testing*, NASA Marshall Space Flight Center, Last Modified on 4.12.06.

[3] M. J. L. Turner, *Rocket and Spacecraft Propulsion Principles*, Practice and New Developments (Third Edition), Praxis Publishing Ltd, Chichester, UK, 2009.

[4] B. Rutan, *SpaceShipOneProgram Summary.* Availabe at www.burtrutan.com, accessed on 28 Dec. 2016.

[5] P. Alergre, P. Sitler, D. Wells, *Space Tourism Business Model The Virgin Galactic Approach*, Availabe at www.geocities.ws, accessed on 28 Dec. 2016.

[6] * * * http://www.spacesafetymagazine.com/aerospace-engineering/rocketry/hybrid-rocket-overview-part-2/

[7] M. Calabro, Overview on Hybrid Propulsion, *Progress in Propulsion Phisics* **2**, EDP Sciences, 2011.

[8] P. L. K. Da Cas, C. Q. Vilanova, M. N. D. Barcelos Jr., C. A. G. Veras, An Optimized Hybrid Rocket Motor for the SARA Platform Reentry System, *J. Aerosp. Technol. Manag.*, São José dos Campos, Vol. **4**, No 3, pp. 317-330, Jul.-Sep., 2012

[9] C. Guță, *Procese termodinamice caracteristice motoarelor rachetă partea I –Motoare rachetă cu combustibil lichid și combinat*, 434 p, București, 1981.

[10] M. Calabro, Overview and History of Hybrid Rocket Propulsion, *Progress in Propulsion Physics* **2**, 353-374, 2011.

[11] G. Cican, A. Mitrache, Rocket Solid Propellant Alternative Based on Ammonium Dinitramide, *INCAS BULLETIN*, volume **9,** Issue 1, (online) ISSN 2247–4528, (print) ISSN 2066–8201, ISSN–L 2066–8201, DOI: 10.13111/2066-8201.2017.9.1.2, pp. 17-24, 2017.

[12] K. K. Rajesh, *Thrust Modulation in a Nitrous- Oxide/Hydroxyl-Terminated Polybutadiene Hybrid Rocket Motor*, 42nd AIAA/ASME/SAE/ASEE Joint Propulsion Conference & Exhibit, 9-12 July 2006, Sacramento, California.

[13] J. Dennis, S. Shark, F. Hernandez, *Design of a N20/HTPB Hybrid Rocket Motor utilizing aToroidal Aerospike Nozzle*, 48th AIAA Aerospace Sciences Meeting Including the New Horizons Forum and Aerospace Exposition 4 - 7 January 2010, Orlando, Florida.

[14] S. M. Chowdhury, *Design and Performance Simulation of a Hybrid Sounding Rocket*, Thesis, December 2012.

[15] J. C. Thomas, E. L. Petersen, *Enhancement of Regression Rates in Hybrid Rockets with HTPB Fuel Grains by Metallic Additives*, AIAA Propulsion and Energy Forum, July 27-29, Orlando, FL, 51st AIAA/SAE/ASEE Joint Propulsion Conference, 2015.

[16] G. P. Sutton and O. Biblarz, *Rocket Propulsion Elements*, 7th ed.,Wiley, NewYork, 2001.

[17] M. J. Chiaverini and K. K. Kuo, Fundaments of Hybrid Rocket Combustion and Propulsion, *AIAA Progress in Astronautics and Aeronautics*, Arlington, Texas, 2007.

[18] M. V. F. Ribeiro, P. C. Greco Junior, *Hybrid Rocket Motors Propellants A Historical Approach*, 21st International Congress of Mechanical Engineering, October 24-28, Natal, RN, Brazil, 2011.

[19] * * * Chemical Equilibrium with Applications, CEA. NASA Computer Program CEA [Online]. Glenn Research Center, Cleveland, OH, United States of America.

[20] * * * Ansys 15 Documentation-User's Guide.

[21] G. Cican, Optimizing a space mission using ion propulsion, *Review of the Air Force Academy*, Vol **XIII**, No 3(30), pp 89-94, (online) ISSN: 2069-4733, 2015.